GEOPHYSICS, VOL. 78, NO. 2 (MARCH-APRIL 2013); P. WA15–WA20, 5 FIGS.
10.1190/GEO2012-0276.1

Low-frequency seismic deghosting

Lasse Amundsen[1] and Hongbo Zhou[2]

ABSTRACT

We evaluated a solution to seismic deghosting that deghosts the low-frequency components of the seismic pressure data. In an approximation that neglected the dependence on wavenumbers, the low-frequency deghosted pressure field was computed trace-by-trace as the sum of the pressure field and its scaled temporally integrated and temporally differentiated fields. We gave simple numerical examples that demonstrated the concept. The method was found to deghost data up to a frequency that is typically half of the second notch frequency. On the low-frequency side, the deghosting method was limited by the signal-to-noise ratio. The low-frequency deghosting technique can be appropriate to apply to the part of seismic data that have penetrated and reflected beneath complex and attenuating overburdens such as basalt, salt, and chalk.

INTRODUCTION

In marine seismic exploration, a source ghost is an event starting its propagation upward from the source, and a receiver ghost ends its propagation moving downward at the receiver. They both have a reflection at the sea surface, which leads to a reduction of the useful frequency bandwidth and therefore damages seismic resolution.

The sea surface ghost reflections modulate the spectrum of conventional pressure seismic data reducing energy at the so-called notch frequencies

$$f_n = \frac{nc}{2z}, \qquad n = 0, 1, 2, \ldots, \tag{1}$$

where c is the speed of sound in water and z is the source or receiver depth. The first notch is always at zero frequency. The second and following notches are steered by depth z. As a result, there is a strong loss of useful low-frequency energy in pressure seismic data, in addition to similar losses at the second and higher notch frequencies. The usable seismic pressure bandwidth is normally between the first and second notch.

The ghost removal process is known as deghosting. Deghosting has been a long-standing problem in the seismic industry but has recently obtained significant industry attention, with proposed solutions that range from new seismic acquisition methods to processing methods that are applicable to conventional data.

Receiver-side deghosting is equivalent to computing the upgoing component of the pressure field, which can be done from measurements of pressure and vertical component of the particle velocity. Several vendors offer such seismic measurements (Vaage et al., 2005; Tenghamn et al., 2007; Caprioli et al., 2012). Receiver-side deghosting techniques for conventional data are described in, e.g., Amundsen (1993), Amundsen et al. (2005), and Weglein et al. (2002), who derive a deghosting method from Green's theorem. Amundsen et al. (2000) apply Green's theorem for deghosting of ocean bottom seismic data. Ramirez and Weglein (2009) give a tutorial on Green's theorem as a comprehensive framework for data reconstruction, regularization, wavefield separation, seismic interferometry, and wavelet estimation.

After receiver-side deghosting, the source ghost is still present in the seismic data. Most published approaches to source deghosting are based on vertical source array acquisition, in which sources are towed in a complex over/under fashion. The reader is referred to the procedures suggested by Moldoveanu (2000, 2001), Moldoveanu et al. (2007), Robertsson et al. (2011), and those published in Vaage (2005). Recently, a so-called ghost-free solution has been introduced based on the GeoSource solution, which requires a time and depth distributed source, using subsources deployed at different depths and fired with specific time delays (Parkes and Hegna, 2011; Petroleum Geo-Services, 2011). Their method removes the source ghost, although mathematically it is not fully wave-theoretically founded because it involves a spectral normalization step at the

Manuscript received by the Editor 17 July 2012; revised manuscript received 3 October 2012; published online 20 March 2013.
[1]Statoil Research Centre, Norway, and The Norwegian University of Science and Technology, Department of Petroleum Engineering and Applied Geophysics, Norway. E-mail: lam@statoil.com.
[2]Statoil Gulf Services, Inc., Houston, Texas, USA. E-mail: hzh@statoil.com.

end. Nevertheless, in practice, this is not a major issue. Further, it has been proposed to apply Green's theorem also for source-side deghosting (see Zhang, 2007; Mayhan et al., 2012).

Although new technologies are being introduced, there is still a pressing need to develop and improve source and receiver deghosting solutions for conventional towed streamer data. The purpose of the present paper is to present a deghosting method that provides greater richness of the low frequencies by tackling the source and receiver ghosts. The technique works with conventional streamer acquisition and so also enables deghosting of legacy data.

Receiver-side deghosting takes place in the common shot domain, whereas source-side deghosting operates in the common receiver domain. In the following, we let the coordinates (x, y) refer to the horizontal spatial variables in a shot gather when addressing receiver-side deghosting, and to the horizontal spatial variables in a receiver gather when addressing source-side deghosting.

A wave theoretical model showing how the ghosts enter the seismic pressure response has been published in, e.g., Amundsen (1993). Mathematically, the ghost functions can be given in the frequency-horizontal wavenumber domain as

$$G(k_x, k_y, k, z) = 1 - r_0 \exp(2ik_z z), \tag{2}$$

where $k_z = \sqrt{k^2 - k_x^2 - k_y^2}$ is the vertical wavenumber; $k = \frac{\omega}{c}$ is the wavenumber for circular frequency $\omega = 2\pi f$, f being the frequency; k_x, k_y are the horizontal wavenumbers conjugate to the horizontal spatial coordinates x, y; and r_0 is the magnitude of the effective reflection coefficient at the sea surface. In the following we assume for simplicity that $r_0 = 1$.

For vertically traveling plane waves, $k_x = k_y = 0$, the ghost function in equation 2 simplifies to

$$G(k_x = k_y = 0, k, z) = G(k, z) = 1 - \exp(2ikz). \tag{3}$$

Its amplitude spectrum is

$$|G(k_x = 0, k_y = 0, k, z)| = 2 \sin(kz). \tag{4}$$

The zeros of the sine-function are the notch frequencies given in equation 1. An example is shown in Figure 1 (solid line) for frequencies up to 150 Hz, where the water speed is 1500 m/s and the depth is 10 m. The three first zeros in the spectrum appear at 0, 75, and 150 Hz.

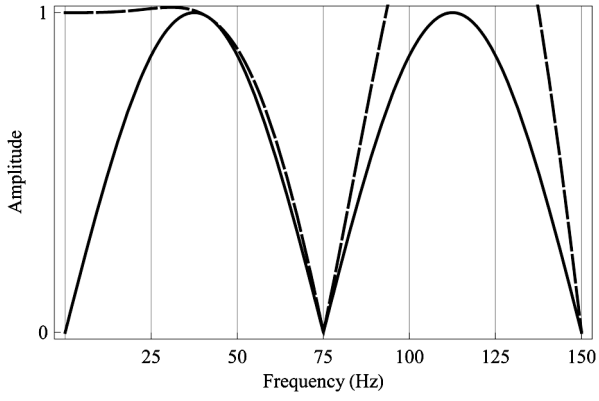

Figure 1. Solid line: Normalized spectrum of the ghost function related to depth 10 m. Dashed line: Spectrum of deghosted data by applying the filter in equation 10 to the data. This filter boosts the low frequencies, typically up to 37.5 Hz. See text for discussion.

In an ideal world, one could remove the ghosts in seismic data in the frequency-wavenumber domain by multiplying the data by the inverse ghost functions, $1/G(k_x, k_y, k, z)$, which for vertically traveling plane waves $k_x = k_y = 0$ reduces to

$$\frac{1}{G(k_x = 0, k_y = 0, k, z)} = \frac{1}{1 - \exp(2ikz)} = \frac{1}{2}[1 + i \cot(kz)]. \tag{5}$$

However, near the notch frequencies, the signal-to-noise ratio (S/N) is usually low, which prevents a successful spectral division. The seismic industry has therefore searched for alternatives to remove the effect of the ghosts.

Here, we offer a method that aims at deghosting the low-frequency components of the seismic measurements. Such a deghosting method can be appropriate to apply to seismic reflection data from below complex and attenuating overburdens such as basalt, salt, or chalk. Because the deghosted data are richer in low frequencies, application of this technique could open up the possibility of improving the performance of other key data processing steps such as velocity model estimation, migration, amplitude variation with offset, inversion, and attribute analysis. In combination, such improvements may lead to better reservoir characterization and thus decrease the risk inherent in seismically driven technical decisions.

We give two remarks: First, the proposed method can be combined with receiver-side deghosting methods that use pressure and particle velocity measurements. The latter approach must handle the typical high levels of flow and vibration noise in towed streamer particle velocity measurements (Vaage et al., 2005; Caprioli et al., 2012) in which the noise on the velocity measurement is stronger than the noise on the pressure measurement at low frequencies. If no action is taken, any noise present on the input particle motion data will directly leak into the deghosted results. One possible solution for cases in which the particle velocity measurement is too noisy is to compute the deghosted data from the pressure measurement (when the S/N is acceptable) using the approach presented here or by using the approach described in Vaage et al. (2005) (see Amundsen, 1993).

Our second remark is related to source-side deghosting methods by using simultaneous source acquisition techniques. At its heart, the simultaneous source method is simple. Consider two sources that are fired simultaneously at every shot location: one being a "master" source shot on position and the other a source fired with prescribed time differences, or dithers, relative to the master. The dithers are randomly distributed over a small time window. A sparse inversion algorithm exploits the source activation times dithered relative to one another to enable separation. Once separated, the data can be deghosted and processed by conventional means. The critical factor is the quality of the source separation. Source firing time dithering may fail to work at low frequencies in which the period is not small compared with the dither times. The proposed deghosting method of the paper might find an application here also.

LOW-FREQUENCY DEGHOSTING

Let the seismic data associated with a source or receiver ghost related to depth z be represented by $U(x, y, \omega, z)$. To find the deghosted data U^{DG}, we apply a filter F to the data U according to

$$U^{DG}(x,y,\omega,z) = F(\partial_x,\partial_y,k,z)U(x,y,\omega,z), \quad (6)$$

where the filter depends on wavenumber k, depth z, and horizontal derivative operators that act on the pressure data (in a common source gather or a common receiver gather). The filter in equation 6 is, in principle, the 2D inverse Fourier transform of the inverse of the ghost function in equation 2. It can be written as a infinite series by performing a series expansion of $1/G$ around $k_x^2 + k_y^2$ before applying the 2D inverse Fourier transform. Therefore, it has an infinite number of approximations, of which a simple one is

$$F(\partial_x,\partial_y,k,z) \approx \frac{1}{2}\left[1 + i\cot(kz) - \frac{iz}{2k}\csc^2(kz)(\partial_x^2+\partial_y^2)\right]. \quad (7)$$

In seismic applications, an approximation that is often made is to neglect the horizontal derivative operators. Then source deghosting is applied trace-by-trace as

$$U^{DG}(\omega,z) \approx F(k,z)U(\omega,z) \quad (8)$$

with

$$F(k,z) = \frac{1}{G(k_x=0,k_y=0,k,z)} = \frac{1}{2}[1 + i\cot(kz)]. \quad (9)$$

Further, in seismic applications in which the focus is to restore the lower frequencies in the seismic data, an approximation to the filter in equation 9 is obtained by keeping the two first terms in the series expansion of the trigonometric function cot

$$F(k,z) \approx \frac{1}{2}\left[1 - \frac{1}{ikz} - \frac{ikz}{3}\right]. \quad (10)$$

When this filter acts on the pressure field, its second term can be interpreted in the time domain as an operator that integrates the pressure in time. Correspondingly, the third term acts as an operator that differentiates the pressure in time. The low-frequency deghosted pressure field is therefore the sum of the pressure field and its scaled temporally integrated and temporally differentiated fields. Thus, in the time domain, trace-by-trace low-frequency deghosting reads

$$U^{DG}(t,z) \approx \frac{1}{2}U(t,z) + \frac{c}{2z}\int_0^t dt' U(t',z) + \frac{z}{6c}\partial_t U(t,z). \quad (11)$$

NUMERICAL EXAMPLES

Deghosting the ghost

The simplest possible demonstration of the low-frequency deghosting concept is to apply the deghosting filter in equation 10 or 11 to the ghost function in equation 3.

The ghost is modeled with $z = 10$ m. The velocity is $c = 1500$ m/s. Considering frequencies up to 150 Hz, the zeros in the frequency spectrum due to the ghost are at $f_0 = 0$ Hz, $f_1 = 75$ Hz, and $f_2 = 150$ Hz. The spectrum of the normalized ghost function is displayed in Figure 1 with the solid line. For this case, the usable bandwidth in real seismic data would be somewhere from 3 to 5 and 75 Hz. We see, however, that the ghost effect has suppressed the amplitudes of the low frequencies significantly. By applying the filter in equation 10 to the ghost function, we obtain the data shown by the dashed line in Figure 1. We observe that the ghost effect for the low frequencies, typically up to $f_1/2 = 37.5$ Hz, is repaired. For frequencies above the second notch at 75 Hz, the filter boosts the amplitudes in the spectrum. This is normally not a problem because boosting takes place outside the usable bandwidth, at frequency amplitudes that will be unused in data processing.

Deghosting simple synthetic data

The next demonstration of the low-frequency deghosting concept is to apply the deghosting filter in equation 11 in the receiver-deghosting mode. Assume that the upgoing field from a deep source at 500 m is measured at a hydrophone at depth $z = 10$ m beneath a free surface. The objective is to repair the effect of the downgoing ghost for low frequencies. The source time function and its amplitude spectrum are shown in Figure 2. Because the modeling is done in 3D, the upgoing signal will be identical to a delayed version of the source time function.

The modeled pressure signal, which is the sum of the upgoing signal and its downgoing ghost, is shown for zero offset in Figure 3a with the long dashed line. The kink seen in the relatively symmetric signal is caused by the ghost. By applying the filter in equation 11 to the signal, we obtain the low-frequency deghosted signal displayed in Figure 3a in the short dashed lines. The corresponding amplitude spectra are shown in Figure 3c. By comparing the amplitude spectrum of the deghosted signal with that of the upgoing signal (see Figure 3c, black line), we see that the deghosting process works

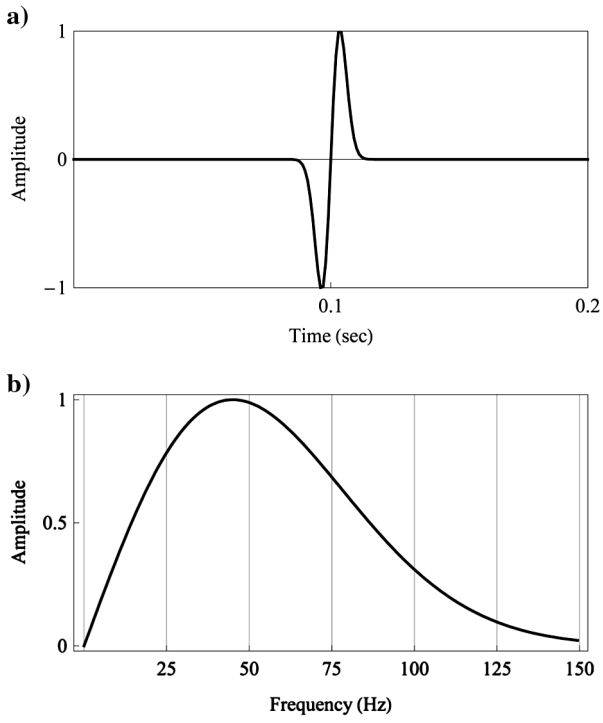

Figure 2. (a) Source time function and (b) its amplitude spectrum.

satisfactorily for low frequencies, up to approximately half of the second notch frequency at 37.5 Hz. High-cut filtering above 75 Hz of the modeled signal and the deghosted signal yields the signatures shown in Figure 3b.

We repeat the modeling exercise but now for a receiver with offset of 250 m. The angle of reflection at the surface is approximately 27°, and the second notch appears at approximately 84 Hz. Again we apply the filter in equation 11 to the signal shown in the long dashed line in Figure 4, and we obtain the low-frequency deghosted signal and the associated amplitude spectrum displayed in the short dashed lines. By comparing the amplitude spectrum of the deghosted signal with that of the upgoing signal (see Figure 4, black line), we see that the deghosting process works quite satisfactorily for low frequencies, even though the angle of incidence is significantly different from zero. To improve the fit, it would be necessary to apply a filter that accounts for the effect of nonzero angles of incidence, for instance, the filter in equation 7.

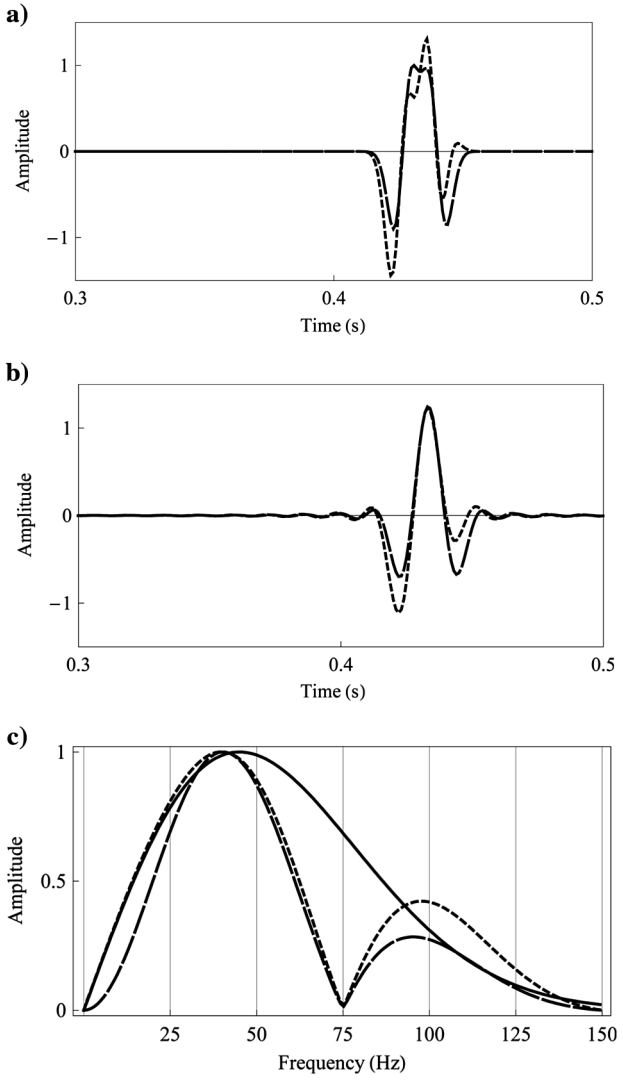

Figure 3. (a) Modeled pressure at zero offset (long dashed line) and low-frequency deghosted pressure (short dashed line). (b) Pressure as in (a) but high-cut filtered above the notch frequency at 75 Hz. (c) Amplitude spectra for data in (a). The amplitude spectrum of the source function in Figure 2 is shown for reference (solid line).

Deghosting synthetic data with added noise

The deghosting method involves the steps of numerical integration and differentiation. Differentiation is a stable process for the low-frequency components of the signal. Integration in the deghosting process, however, will depend on the S/N at low frequencies.

We have demonstrated the deghosting method on synthetic data. Of course, deghosting of real data is a more tricky matter. It is outside the scope of the present paper to investigate thoroughly how the deghosting method tackles noise because its performance will depend on the particular integration method and the type of noise. But, the method will suffer the same S/N problems at the low-frequency end as conventional deghosting methods will. However, at the high-frequency end, closer to the second notch, the method is less sensitive to low S/Ns.

Although not very realistic, we give an example of low-frequency deghosting when noise is added to the synthetic data in the zero-offset example above. The noise is a white noise sequence that is designed in the frequency domain and has zero mean in the time domain.

Figure 5a and 5b displays the noisy signal and its associated amplitude spectrum shown up to 75 Hz in the dashed lines. The noise-free signal is plotted in Figure 3a, and its amplitude spectrum is reproduced in Figure 5b in the solid line. Comparing the spectra,

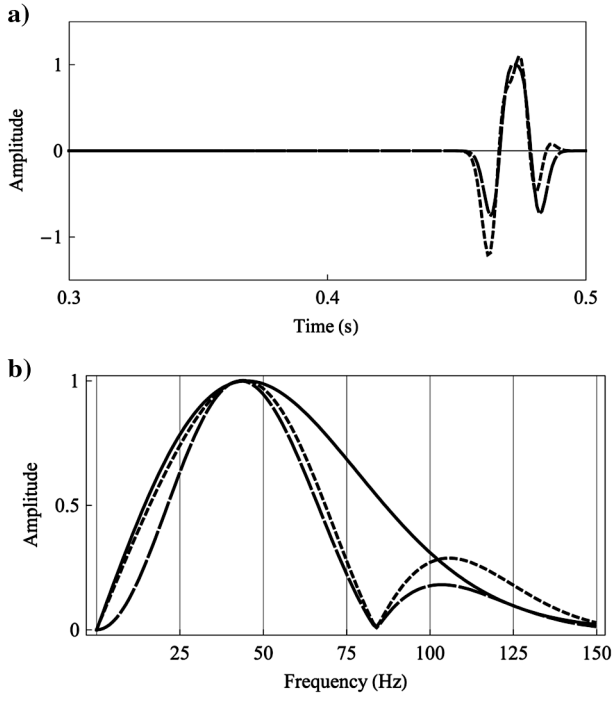

Figure 4. (a) Modeled pressure at offset 250 m (long dashed line) and low-frequency deghosted pressure (short dashed line) and (b) associated amplitude spectra. The amplitude spectrum of the source function in Figure 2 is shown for reference (solid line). The source is located at depth 500 m, such that the receiver ghost is reflected at an angle of approximately 27°. The notch frequency is at approximately 84 Hz.

we see that below around 10 Hz, the noise level is significantly above the signal level, except at zero frequency, where the signal and noise have zero amplitude. (Both the source signature and the noise have zero energy at zero Hz.)

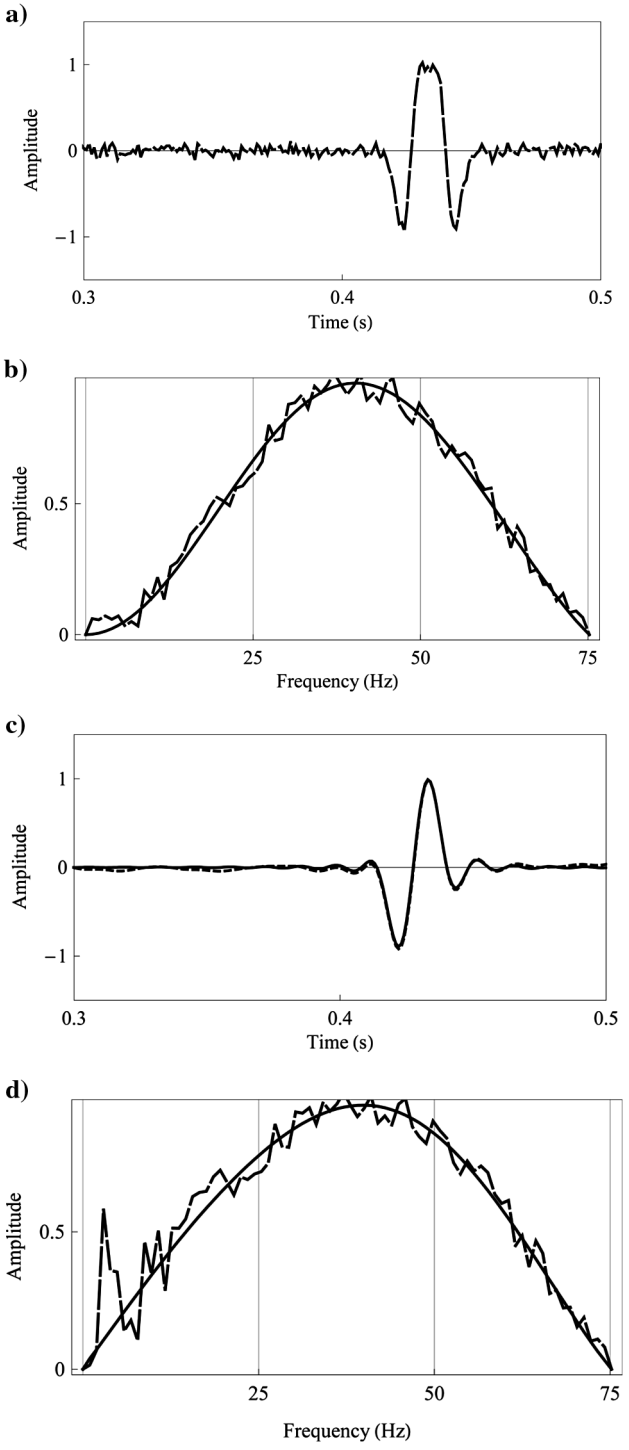

Figure 5. Displayed with dashed lines: (a) Noisy data, (b) associated amplitude spectrum shown for 0–75 Hz, (c) deghosted data high-cut filtered above 75 Hz, and (d) associated amplitude spectrum. The noise-free data are displayed in Figure 3a. The solid lines in (b)-(d) show the corresponding results for noise-free data.

When applying the low-frequency deghosting method to the noisy data, we use a 3 Hz low-cut filter in the integration (summation). In addition, we apply a high-cut filter to the deghosted signal above 75 Hz. The result of the deghosting method is shown in the time domain with the dashed line in Figure 5c. The amplitude spectrum is given in Figure 5d. Compared with the noise-free results (solid lines), we observe that the low-frequency part of the noise, between 3 and 10 Hz, has been blown up due to the numerical integration of the noise. The deghosted time trace, however, compares well with the noise-free deghosted time trace as seen in Figure 5c.

CONCLUSION

We have presented a solution to deghosting that deghosts the low-frequency components of the seismic pressure data, typically up to a frequency that is half of the second notch frequency. The low-frequency deghosted pressure field can be computed as the sum of the pressure field and its scaled temporally integrated and temporally differentiated fields. The method is limited by the S/N at the low-frequency side.

ACKNOWLEDGMENTS

We thank Statoil for permission to publish these results and the reviewers (R. Laws, D.-J. van Manen, and one anonymous) for constructive comments that helped improve the paper.

REFERENCES

Amundsen, L., 1993, Wavenumber-based filtering of marine point-source data: Geophysics, **58**, 1335–1348, doi: 10.1190/1.1443516.
Amundsen, L., L. T. Ikelle, and J. Martin, 2000, Multiple attenuation and P/S splitting of multicomponent OBC data at a heterogeneous sea floor: Wave Motion, **32**, 67–78, doi: 10.1016/S0165-2125(99)00047-5.
Amundsen, L., T. Røsten, J. O. A. Robertsson, and E. Kragh, 2005, On rough-sea deghosting of streamer seismic data using pressure gradient approximations: Geophysics, **70**, no. 1, V1–V9, doi: 10.1190/1.1852892.
Caprioli, P., K. Özdemir, D. J. van Manen, S. Mahat, A. Özbek, E. Kragh, and P. Christie, 2012, Combination of multi-component streamer pressure and vertical particle velocity — Theory and application to data: 82nd Annual International Meeting, SEG, Expanded Abstracts, 1–5.
Mayhan, J. D., P. Terenghi, A. B. Weglein, and N. Chemingui, 2012, First use of Green's theorem derived source side deghosting on deep water Gulf of Mexico synthetic and field data: 82nd Annual International Meeting, SEG, Expanded Abstracts, 31.
Moldoveanu, N., 2000, Vertical source array in marine seismic exploration: 70th Annual International Meeting, SEG, Expanded Abstracts, 53–56.
Moldoveanu, N., 2001, A seismic source, a marine seismic surveying arrangement, a method of operating a marine seismic source, and a method of deghosting seismic data: Australian Patent WO 01/75481.
Moldoveanu, N., L. Combee, M. Egan, G. Hampson, L. Sydora, and W. Abriel, 2007, Over/under towed streamer acquisition: A method to extend seismic bandwidth to both higher and lower frequencies: The Leading Edge, **26**, 41–58, doi: 10.1190/1.2431831.
Parkes, G., and S. Hegna, 2011, A marine seismic acquisition system that provides a full "ghost-free" solution: 81st Annual International Meeting, SEG, Expanded Abstracts, 37–41.
Petroleum Geo-Services, 2011, GeoStreamer GS™ — The ghost free solution: PGS Tech Link, **11**, no. 4, 1–4.
Ramirez, A. C., and A. B. Weglein, 2009, Green's theorem as a comprehensive framework for data reconstruction, regularization, wavefield separation, seismic interferometry, and wavelet estimation: A tutorial: Geophysics, **74**, no. 6, W35–W62, doi: 10.1190/1.3237118.
Robertsson, J. O. A., D.-J. van Manen, D. Halliday, and R. Laws, 2011, Seismic data acquisition and source-side derivatives generation and application: U. S. Patent 7,876,642.
Tenghamn, R., S. Vaage, and C. Borresen, 2007, A dual-sensor towed marine streamer: Its viable implementation and initial results: 77th Annual International Meeting, SEG, Expanded Abstracts, 989–993.

Vaage, S. T., 2005, Method and system for acquiring marine seismic data using multiple seismic sources: U. S. Patent 6,906,981.
Vaage, S. T., S. T. L. Tenghamn, and C. N. Borresen, 2005, System for combining signals of pressure sensors and particle motion sensors in marine seismic streamers: U. S. Patent 0,195,686.
Weglein, A. B., S. A. Shaw, K. H. Matson, J. L. Sheiman, R. H. Solt, T. H. Tan, A. Osen, G. P. Correa, K. A. Innanen, Z. Guo, and J. Zhang, 2002, New approaches to deghosting towed-streamer and ocean-bottom pressure measurements: 72nd Annual International Meeting, SEG, Expanded Abstracts, 1016–1019.
Zhang, J., 2007, Wave theory based data preparation for inverse scattering multiple removal, depth imaging and parameter estimation: Analysis and numerical tests of Green's theorem deghosting theory: Ph.D. thesis, University of Houston.